Int. J. Heat Mass Transfer. Vol. 36, No. 3, pp. 755–763, 1993
Printed in Great Britain

0017-9310/93 $6.00+0.00

Natural convection heat transfer in enclosures fitted with a periodic array of hot roughness elements at the bottom

M. RUHUL AMIN
Department of Mechanical Engineering, Montana State University, Bozeman, MT 59717, U.S.A.

(*Received* 25 *July* 1991 *and in final form* 7 *January* 1992)

Abstract—The natural convection heat transfer in a two-dimensional rectangular enclosure fitted with a periodic array of hot roughness elements at the bottom is investigated numerically. The numerical investigation is carried out for the ranges of Rayleigh numbers (Ra_H) and aspect ratios (W/H) from 10^2 to 10^5 and from 1.0 to 4.0, respectively, at a Prandtl number (Pr) of 0.707. Increase in heat transfer is obtained when the roughness element phase shift is equal to half its period. The increment in heat transfer is more significant for enclosures with higher values of roughness element amplitude. The highest value of heat transfer enhancement obtained in this research is 78%. This is obtained for an enclosure with $W/H = 4.0$ at $Ra_H = 10^2$.

INTRODUCTION

NATURAL convection heat transfer in fluid-filled enclosures has received considerable attention because of its diverse practical applications. Most of the previous work is focused in the area where the natural convective flow is generated due to either a vertical or horizontal temperature difference or imposed heat flux. For the enclosure heated from the side, the fluid motion starts for a very small temperature difference across the layer. On the other hand, for the enclosure heated from below, the fluid motion does not start until a critical value of temperature difference across the fluid layer is achieved.

Little work has been done for the more complex boundary condition, where the natural convection flow is generated due to the temperature difference between a hot horizontal wall and an adjacent cold vertical wall. This type of flow has important application in the heat transfer analyses of electronic equipment, specifically the so-called slim rack as described by Carvalho *et al.* [1], where the rate of power dissipation from the horizontal circuit board is limited by its temperature. Other applications include the design of energy efficient buildings, solar collectors, fluid-filled thermal storage tanks, operation and safety of nuclear reactors, and fire prevention and safety.

Torrance and Rockett [2] performed a numerical study of the convective flow of air in a vertical cylindrical enclosure. The side wall of the cylinder was cooled while a small spot was heated at the center of the bottom surface. The authors found that for a Grashof number greater than 10^6, the flow inside the enclosure is dominated by a rising column of hot fluid just above the hot spot and confined around a vertical axis of the cylinder. The authors concluded that for Grashof numbers greater than 4×10^6, a large thermally stratified region develops inside the cylindrical enclosure. The same geometry was investigated experimentally by Torrance *et al.* [3] and a similar numerical study was performed by Greenspan and Shultz [4]. Shiralkar and Tien [5] performed a numerical study on the convective heat transfer in a rectangular enclosure with the vertical and horizontal temperature gradients applied simultaneously. They found that a stabilizing vertical temperature decreases the vertical velocity of the fluid near the hot wall and increases the horizontal heat transfer. The authors also reported that for a destabilizing temperature difference, effective horizontal heat transfer occurs from the cold wall to the hot wall with high enough values of the vertical heat flux. Chao *et al.* [6] performed a combined experimental and numerical study of the natural convection heat transfer in a rectangular enclosure. The vertical sides of the enclosure were insulated, the top wall was cooled while half the bottom surface was heated and the other half was insulated. The authors reported that a single pair of rolls develops when half the bottom wall is heated. They also reported that for any value of temperature difference, a convective motion of the fluid is generated and the rate of heat transfer is higher than that of pure conduction.

Kimura and Bejan [7] studied the natural convection flow in a differentially heated corner region. The bottom horizontal wall was cooled and one of the adjacent vertical walls was heated in their investigation. They used both isothermal and constant heat flux boundary conditions. In the asymptotic part of their solution, the authors showed that for $Ra_H \to 0$, the flow field is relatively insensitive to the boundary conditions. The authors concluded in the numerical part of their solution that with the increase of Rayleigh number, the single-cell flow inside the enclosure draws near the intersection of the cold wall and hot

NOMENCLATURE

A^*	amplitude of roughness element, see Fig. 1
A	dimensionless amplitude of roughness element, A^*/H
C_p	constant pressure specific heat of fluid
g	magnitude of acceleration due to gravity
H	height of the enclosure
k	thermal conductivity of fluid
$\overline{Nu}_R$	average Nusselt number of an enclosure containing roughness elements
$\overline{Nu}_S$	average Nusselt number of a smooth-walled enclosure
P^*	motion pressure
P	dimensionless motion pressure, $P^*H^2/\rho\nu^2$
Pr	Prandtl number, $\mu C_p/k$
Ra_H	Rayleigh number, $g\beta(T_H^*-T_C^*)H^3/\nu\alpha$
T^*	temperature
T	dimensionless fluid temperature, $(T^*-T_C^*)/(T_H^*-T_C^*)$
T_f^*	see equation (1)
T_H^*	hot wall temperature
T_0	$(T_H^*-T_C^*)/T_C^*$
T_C^*	cold wall temperature
u^*	x^*-component of velocity
u	dimensionless x-component of velocity, u^*H/ν
v^*	y^*-component of velocity
v	dimensionless y-component of velocity, v^*H/ν
W	width of enclosure
x^*, y^*	spatial coordinates, see Fig. 1
x, y	dimensionless spatial coordinates, x^*/H, y^*/H.

Greek symbols

α	thermal diffusivity of fluid
β	coefficient of thermal expansion of fluid
δ^*	period of roughness elements
δ	dimensionless period of roughness elements, δ^*/H
ε^*	length of the part of the bottom wall which is adiabatic, see Fig. 1
ε	dimensionless length of the part of the bottom wall which is adiabatic, ε^*/H
μ	dynamic viscosity of fluid
ν	kinematic viscosity of fluid
ρ	density of fluid
ϕ^*	phase shift of rectangular roughness elements
ϕ	dimensionless phase shift of rectangular roughness elements, ϕ^*/H
ψ	dimensionless stream function, defined by equations (5) and (6).

wall. Thermal stratification of the enclosed fluid was observed in their study. Poulikakos [8] performed a numerical study on the natural convection in a rectangular enclosure with heated and cooled regions on a single vertical wall. The other three walls of the enclosure were kept adiabatic. The author reported that intense convective motion and heat transfer occur inside the enclosure when the lower portion of the vertical wall is heated and the upper portion is cooled. The fluid motion and heat transfer rate is less intense when the condition is reversed; that is, the lower portion of the vertical wall is cooled and the upper portion is heated. Anderson and Lauriat [9] performed a study in a square enclosure with uniform heat flux or isothermal (hot) bottom horizontal wall. One of the vertical walls was cooled and the other two walls of the enclosure were maintained adiabatic. A single cell flow with stable boundary layer adjacent to the heated wall was observed in their study. November and Nansteel [10] performed an analytical and numerical study of the natural convection in a rectangular enclosure filled with water for $0 \leqslant Ra_H \leqslant 10^6$. The bottom horizontal wall of their enclosure was partly heated and partly adiabatic while one of the vertical walls was cooled. The other two walls of the enclosure were kept adiabatic. They reported that a single cell of fluid motion occurs with strong thermal boundary layers adjacent to the hot and cold walls for a value of Rayleigh number of about 10^5. The authors concluded that convective heat transfer is most significant when little less than half the bottom horizontal surface is heated. Most recently Granzarolli and Milanez [11] performed a numerical study of the natural convection in a rectangular enclosure heated from below and cooled symmetrically from the two vertical sides. Their study was performed in the range of Rayleigh numbers from 10^3 to 10^6 and for Prandtl numbers of 0.7 and 7.0. A correlation for the Nusselt number with Rayleigh number is reported. The authors concluded that Prandtl number has very little effect on the Nusselt number.

None of the studies discussed above has investigated the natural convection heat transfer mechanism in an enclosure fitted with a periodic array of roughness elements on the bottom hot horizontal wall. Therefore, the objective of the present research is to find the effects of mounting a periodic array of large rectangular roughness elements on a partly hot and partly adiabatic bottom horizontal wall of a two-dimensional rectangular enclosure. The enclosure is filled with a Newtonian fluid. The left vertical wall and the top horizontal wall are maintained adiabatic. Part of the bottom horizontal wall is maintained iso-

thermal at a temperature of T_H^* and the right vertical wall is maintained isothermal at a temperature of T_C^* ($T_H^* > T_C^*$). A portion of the bottom horizontal wall of length ε^*, adjacent to the cold vertical wall, is maintained adiabatic. This is done to avoid any singularity as described by Nansteel *et al.* [12], at the intersection of the hot horizontal and cold vertical walls. In this study, the length, ε^*, is chosen so that the dimensionless length of the adiabatic portion of the bottom wall (ε) is always maintained at a constant value of 0.1.

Two basic geometries as shown in Fig. 1 are investigated in this study. The enclosure shown in Fig. 1(a) has smooth walls and is used in this research to find the effects of placing a periodic array of large rectangular roughness elements on the bottom wall of the enclosure. The roughness elements on the bottom horizontal wall as shown in Figs. 1(b) and (c) were designed such that the volume of the fluid in the rough-walled enclosure remained the same as the volume of the fluid in the corresponding smooth-walled enclosure. This is necessary for this investigation because merely attaching large roughness elements on the horizontal wall will appreciably reduce the effective height (see Figs. 1(b) and (c)) and as such increase the aspect ratio of the enclosure. It is shown later that for the present enclosures shown in Fig. 1, the heat transfer rate decreases as the aspect ratio increases. Therefore, merely attaching large roughness elements on the horizontal wall without keeping the volume of the enclosure the same as the corresponding smooth-walled enclosure would increase the aspect ratio of the rough-walled enclosure. This effect would preclude an equitable comparison between the corresponding enclosures with smooth walls and rough walls.

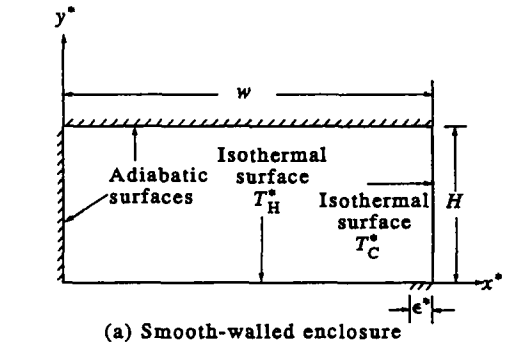

(a) Smooth-walled enclosure

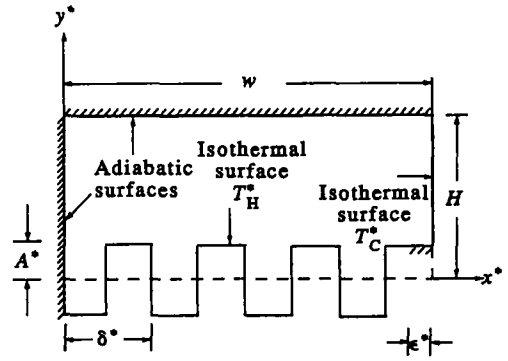

(b) Rough-walled enclosure with $\phi^* = 0$

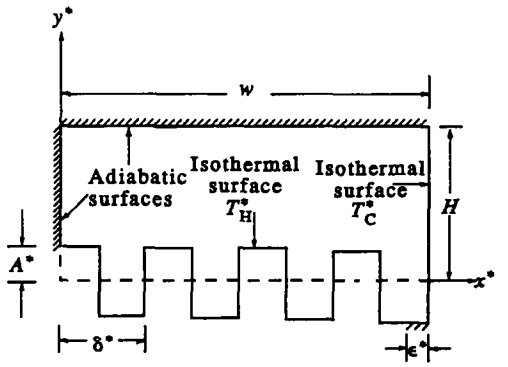

(c) Rough-walled enclosure with $\phi^* = \delta^*/2$

FIG. 1. Investigated enclosure geometries.

MATHEMATICAL FORMULATION

Modeling assumptions

In the present work it is assumed that the natural convection flows of the Newtonian fluids in the enclosures of interest are steady-state, two-dimensional, and laminar. It is also assumed that the volume of the fluid in the rough-walled enclosure is the same as that of the corresponding smooth-walled enclosure, that the Boussinesq approximation is valid, that the fluid is a radiatively nonparticipating medium, and that viscous dissipation and compressive work are negligibly small.

As suggested by Zhong *et al.* [13], the fluid properties in this research were evaluated at a temperature, T_f^*, which is expressed as

$$T_f^* = T_C^* + 0.25(T_H^* - T_C^*). \tag{1}$$

For the validity of Boussinesq approximation, in this research the temperature difference between the hot and cold walls was chosen such that $T_0 \leqslant 0.1$ [13], where $T_0 = (T_H^* - T_C^*)/T_C^*$.

The governing equations

Based on the above modeling assumptions, the nondimensional governing equations for the conservation of mass, momentum, and energy are

$$\frac{\partial u}{\partial x} + \frac{\partial v}{\partial y} = 0 \tag{2a}$$

$$u\frac{\partial u}{\partial x} + v\frac{\partial u}{\partial y} = -\frac{\partial P}{\partial x} + \frac{\partial^2 u}{\partial x^2} + \frac{\partial^2 u}{\partial y^2} \tag{2b}$$

$$u\frac{\partial v}{\partial x} + v\frac{\partial v}{\partial y} = -\frac{\partial P}{\partial y} + \frac{\partial^2 v}{\partial x^2} + \frac{\partial^2 v}{\partial y^2} + \frac{Ra_H}{Pr}T \tag{2c}$$

$$u\frac{\partial T}{\partial x} + v\frac{\partial T}{\partial y} = \frac{1}{Pr}\left(\frac{\partial^2 T}{\partial x^2} + \frac{\partial^2 T}{\partial y^2}\right) \tag{2d}$$

where P, the 'motion pressure', is defined as the actual pressure in the fluid less the pressure when the fluid is at rest at the reference temperature. The temperature of the cold vertical wall of the enclosure, T_C^*, serves as the reference temperature in the buoyancy force term in equation (2c).

The corresponding boundary conditions are described as follows:

$$u = v = 0, \text{ on all solid walls} \tag{3a}$$

$$\frac{\partial T}{\partial x} = 0, \text{ on left vertical wall} \tag{3b}$$

$$\frac{\partial T}{\partial y} = 0, \text{ on top horizontal wall} \tag{3c}$$

$$T = 0, \text{ on right vertical wall} \tag{3d}$$

$$T = 1 \text{ (for } 0 \leqslant x \leqslant W/H - \varepsilon), \text{ on bottom horizontal wall} \tag{3e}$$

$$\frac{\partial T}{\partial y} = 0 \text{ (for } W/H - \varepsilon \leqslant x \leqslant W/H), \text{ on bottom horizontal wall.} \tag{3f}$$

The nondimensional form of the stream function can be expressed as

$$\frac{\partial^2 \psi}{\partial x^2} + \frac{\partial^2 \psi}{\partial y^2} = \frac{\partial u}{\partial y} - \frac{\partial v}{\partial x} \tag{4}$$

where the stream function ψ is defined by

$$u = \frac{\partial \psi}{\partial y} \tag{5}$$

$$v = -\frac{\partial \psi}{\partial x}. \tag{6}$$

The impermeability and zero tangential velocity slip on the solid walls require that

$$\psi = \partial \psi / \partial n = 0, \text{ on the boundary.} \tag{7}$$

Heat transfer

The overall heat transfer across the enclosure is expressed in terms of the average Nusselt number. This quantity is easily computed after a solution of the governing equations has been completed. The computation merely involves the integration of the local Nusselt number distribution along either the isothermal cold vertical wall or the isothermal hot portion of the bottom horizontal wall. For convenience, the cold vertical wall is chosen for this purpose since it is always a plane surface, even in an enclosure containing roughness elements. The average Nusselt number in nondimensional form is defined as

$$\overline{Nu}_R = \int_A^1 -\frac{\partial T(W/H, y)}{\partial x} \, dy \tag{8a}$$

for $\phi = 0$ (Fig. 1(b)), and

$$\overline{Nu}_R = \int_{-A}^{1} -\frac{\partial T(W/H, y)}{\partial x} \, dy \tag{8b}$$

for $\phi = \delta/2$ (Fig. 1(c)). The above integrals are evaluated using Simpson's rule.

NUMERICAL PROCEDURE

The governing equations for the present study were solved by using the finite element code NACHOS II, developed by Gartling [14, 15]. This is a general purpose finite element code designed to solve the two-dimensional Navier–Stokes and energy equations for both steady-state and transient flows. A detailed description of the code has been documented elsewhere [14, 15], and will not be discussed here.

The finite element grids used by NACHOS II were different for different geometries of the enclosures. The elements were arranged such that more of them were packed into regions of large gradients of velocity and/or temperature. The grids were generated by the internal grid generator of the code. It should be noted here that the grid generator of the code can generate nine grid points for each element, four at the corner points of the element, one at the center of each side of the element (total of four), and one grid point at the center of the element.

RESULTS AND DISCUSSIONS

As reported earlier, the numerical solution of the present research was performed by using the finite element code, NACHOS II. To check the accuracy of the code for the present problem, several cases were run at different values of Rayleigh number for a smooth-walled enclosure (Fig. 1(a)) with an aspect ratio $(W/H) = 1.0$, $\varepsilon = 0.5$, and at $Pr = 6.7$. The computed values of average Nusselt numbers ($\overline{Nu}_S$) for these cases were compared with the corresponding results of November and Nansteel [10]. This comparison is shown in Fig. 2 from which it can be seen

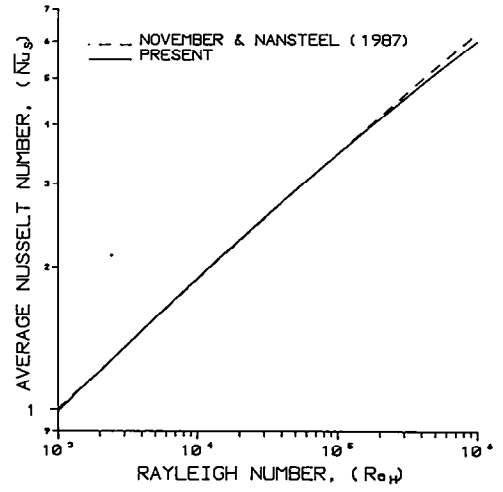

FIG. 2. Comparison of the numerical accuracy of the present method for a smooth-walled enclosure with $W/H = 1.0$, $\varepsilon = 0.5$, and $Pr = 6.7$.

that the results obtained by the present method are in good agreement with other published results.

From the nondimensional governing equations and boundary conditions it can be seen that the average Nusselt number ($\overline{Nu}_R$) for the rough-walled enclosure has the following functional dependencies:

$$\overline{Nu}_R = \overline{Nu}_R(Ra_H, Pr, W/H, A, \delta, \phi, \varepsilon). \quad (9)$$

In this research the values of Pr and ε were kept constant at 0.707 and 0.1, respectively. The range of Rayleigh numbers (Ra_H) considered was from 10^2 to 10^5. Higher values of Ra_H could not be investigated due to the limitation of computer resources. The complex nature of the boundary conditions of the present research requires extremely long computer time to obtain a stable solution. Results are presented for the range of aspect ratios (W/H) from 1.0 to 4.0. High values of aspect ratios were chosen because it would closely resemble the circuit cards of electronic equipment. Roughness element amplitudes (A) of 0.125 and 0.25, periods (δ) of 0.5 and 1.0, and phase shifts (ϕ) of 0 and $\delta/2$ were considered in this study.

The rate of heat transfer by natural convection in the smooth-walled enclosure (Fig. 1(a)) was determined to study the effects of placing large roughness elements in a corresponding rough-walled enclosure. Results are presented in this research as the ratio of the average Nusselt numbers of the rough and smooth-walled enclosures ($\overline{Nu}_R/\overline{Nu}_S$).

Figure 3† shows the streamlines and isotherms for an enclosure with $W/H = 4.0$, $A = 0.25$, $\delta = 0.5$, $\varepsilon = 0.1$, $\phi = \delta/2$, at $Pr = 0.707$ and for $Ra_H = 10^3$, 10^4, and 10^5. The arrows show the locations of the corresponding smooth-walled enclosure. This figure shows that: (1) heat transfer inside the enclosure is dominated by conduction at low value of Ra_H and by convection at high value of Ra_H, (2) the cavities created by the roughness elements remain convectively inactive (no fluid motion), except the one adjacent to the cold wall, and (3) at low values of Ra_H, a large section of the left hand portion of the cavity remains convectively inactive.

In this research heat transfer enhancement is observed in a rough-walled enclosure, that is $(\overline{Nu}_R/\overline{Nu}_S) > 1$, when the roughness elements are mounted so that the phase shift, $\phi = \delta/2$ (Fig. 1(c)). On the other hand, heat transfer decreases, that is $(\overline{Nu}_R/\overline{Nu}_S) < 1$, when the roughness elements are mounted with $\phi = 0$ (Fig. 1(b)). This effect can be seen in Fig. 4 where curve A is compared with curve B, and curve C with curve D. The reason for this trend can be explained with the help of Fig. 3. It can be seen from Fig. 3 that when $\phi = \delta/2$, the length of the cold wall is increased in comparison with that of a corresponding smooth-walled enclosure. The total heat transfer across the enclosure is the amount of heat that is transferred from the hot wall to the cold wall via the fluid inside the enclosure. So, the length of the cold wall is one of the factors which controls how much heat can be transferred from the hot wall to the cold wall. Therefore, when the length of the cold wall is increased due to the mounting of roughness elements (by an amount equal to the amplitude length, A), the heat transfer rate is expected to increase. It is also important to note that the maximum amount of heat transfer from the hot wall occurs from the section of the hot wall which is adjacent to the cold vertical wall; that is, when $\phi = \delta/2$, it is the first cavity from the right. This section of the hot wall has higher value of temperature gradient, which can be verified from Fig. 3 by noting higher concentration of isotherms in the first roughness element cavity adjacent to the cold wall. When $\phi = \delta/2$ in a rough-walled enclosure, the length of the hot wall with higher temperature gradient is greater than that of a corresponding smooth-walled enclosure. So, enhancement of heat transfer occurs in the rough-walled enclosure. Also when $\phi = \delta/2$, a cavity adjacent to the cold wall, with vertical and closely spaced hot and cold walls is created. The creation of such a cavity increases the heat transfer both at low and high Rayleigh numbers in comparison to the smooth wall case. These factors contribute to the enhancement of heat transfer when $\phi = \delta/2$. However, when $\phi = 0$ (Fig. 1(b)), it is the opposite. In this geometry, the lengths of the cold wall and the high temperature gradient region of the hot wall are smaller than that of a corresponding smooth-walled enclosure. Also no cavity is created adjacent to the cold wall. Therefore, reduction in heat transfer occurs.

It can also be seen from Fig. 4 that the heat transfer enhancement (when $\phi = \delta/2$) is more in the conduction dominated cases (low values of Ra_H) than that of the convection dominated cases (high values of Ra_H). This is expected because the amount of heat transfer by conduction for a particular temperature difference is inversely proportional to the effective distance between the hot and cold walls. As can be seen from the streamlines of Fig. 3, there is no fluid motion inside the cavities created by the roughness elements except the one adjacent to the cold wall. These cavities, except the one adjacent to the cold wall, are isothermal and have the same temperature as that of the hot wall. This reduces the effective height of the enclosure and, as such, reduces the distance between the hot and cold walls. Therefore, higher values of heat transfer enhancement are observed in conduction dominated cases.

To explore the effect of aspect ratio on the overall heat transfer across the enclosure, several cases were run. It is observed that for both smooth-walled and rough-walled enclosures, the heat transfer increases with the increase of aspect ratio. However, past a critical value of the aspect ratio, the heat transfer across the enclosure remains almost constant except

† In Figs. 3, 6, and 7 the notation $T = 0(0.1)1$ for the isotherms indicates that these contours are plotted for nine equally spaced values of T between zero and unity.

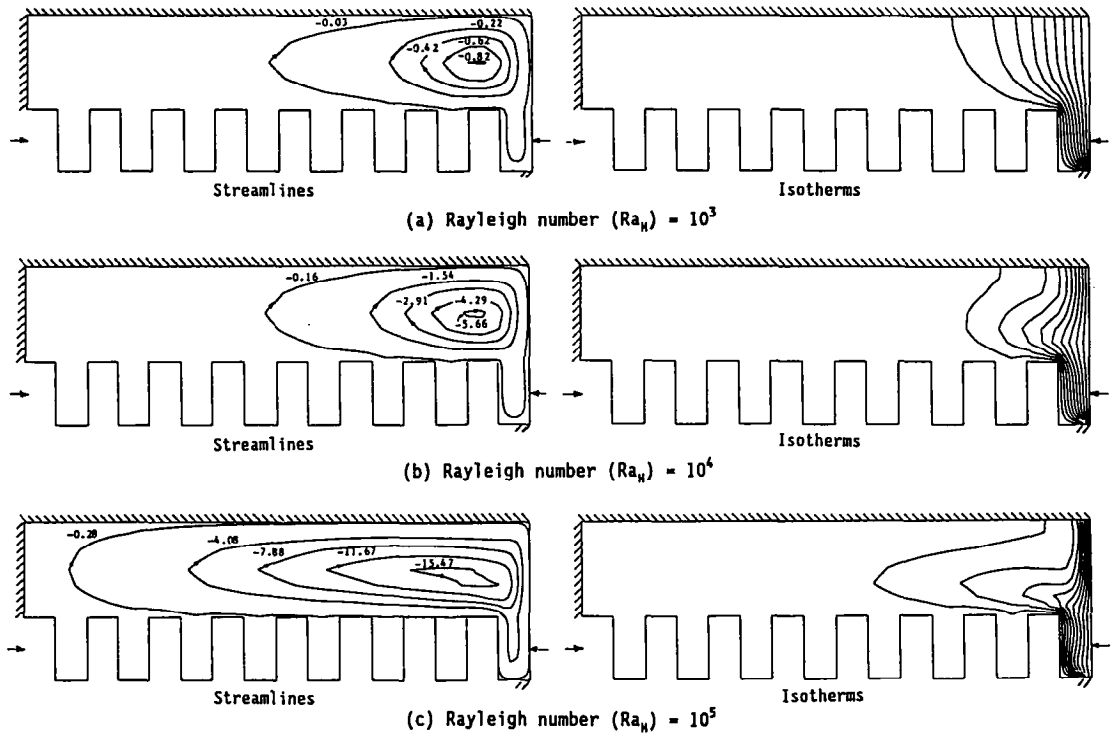

FIG. 3. Computed streamlines and isotherms, $T = 0(0.1)1$, in a rough-walled enclosure with $W/H = 4.0$, $A = 0.25$, $\delta = 0.5$, $\varepsilon = 0.1$, $\phi = \delta/2$, and $Pr = 0.707$.

at high values of Ra_H (convection dominated flow). This trend is clearly visible in Fig. 5 where the average Nusselt numbers ($\overline{Nu}_R$) for enclosures with $A = 0.25$, $\delta = 1.0$, $\phi = \delta/2$, $\varepsilon = 0.1$ for different values of aspect ratios (W/H) and Rayleigh numbers (Ra_H) are plotted. In an attempt to have a reasonable explanation for this trend, Figs. 6 and 7 are introduced. These two figures show the streamlines and isotherms for enclosures with $A = 0.25$, $\delta = 1.0$, $\varepsilon = 0.1$ for values of aspect ratios (W/H) = 1.0, 2.0, and 4.0 and for $Ra_H = 10^3$ and 10^5. The arrows show the locations of the corresponding smooth wall. From the streamline and isotherm contours of Figs. 6(b) and (c), we can see that although the total area of the enclosure is increased with the increase of aspect ratio from 2.0 to 4.0, the thermally active areas of these two

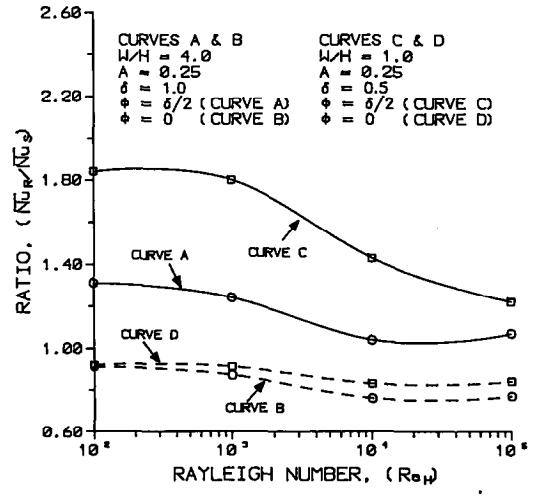

FIG. 4. The effect of phase shift on the ratio of Nusselt numbers for enclosures with $Pr = 0.707$.

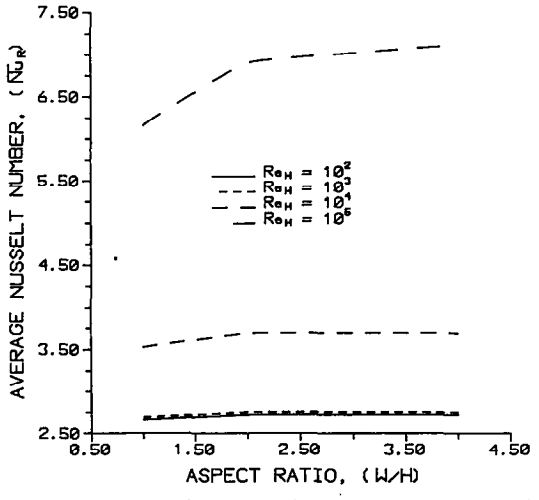

FIG. 5. The effect of aspect ratio on the average Nusselt number for rough-walled enclosures with $A = 0.25$, $\delta = 1.0$, $\varepsilon = 0.1$, and $Pr = 0.707$.

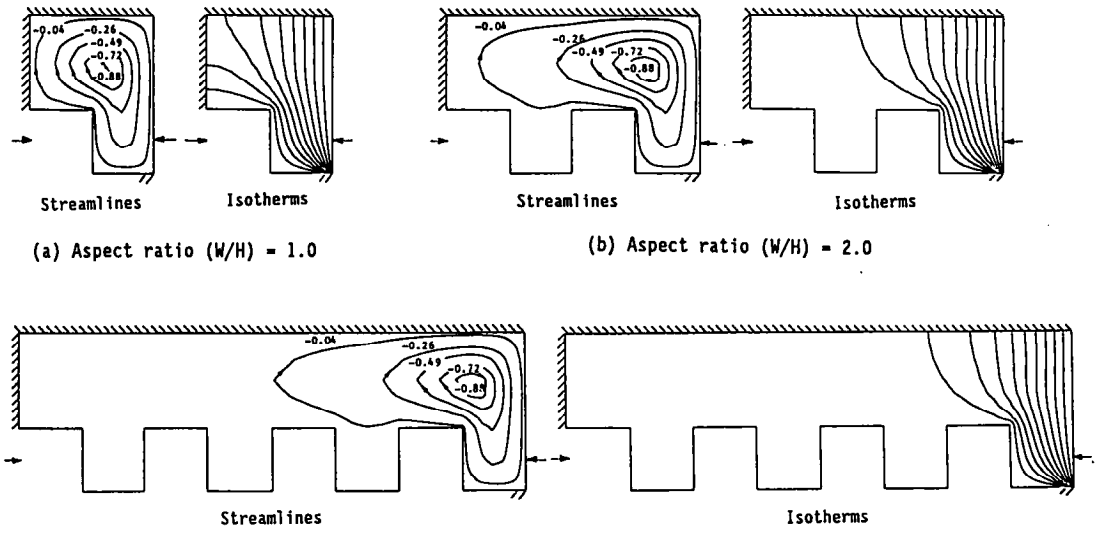

FIG. 6. Computed streamlines and isotherms, $T = 0(0.1)1$, for enclosures with $A = 0.25$, $\delta = 1.0$, $\varepsilon = 0.1$, and $Ra_H = 10^3$.

enclosures remain almost the same. The left portions of these enclosures are isothermal and there is no heat transfer either by conduction or convection. It should be noted, however, that these active areas are higher than that of Fig. 6(a) (with $W/H = 1.0$). Hence, at low values of Ra_H, when the aspect ratio is increased beyond a critical value, the heat transfer rates remain constant. On the other hand, if we examine Fig. 7 we can see that at high values of Ra_H, thermally active areas of the enclosures increase with the increase of enclosure aspect ratio. In fact, in these cases the entire enclosure becomes thermally active except for a few cavities created by the roughness elements. Therefore, increase in heat transfer with the increase of aspect ratio is expected at high Ra_H flow.

Figure 8 shows the effect of changing the amplitude, A, of the roughness elements for enclosures with $W/H = 4.0$, $\varepsilon = 0.1$, $\phi = \delta/2$ and for values of $\delta = 0.5$ and 1.0. Results are presented as the ratio of Nusselt numbers ($\overline{Nu}_R/\overline{Nu}_S$) and the amplitude is changed from 0.125 to 0.25 at various values of Ra_H. To study the effect of amplitude from this figure, curve A should

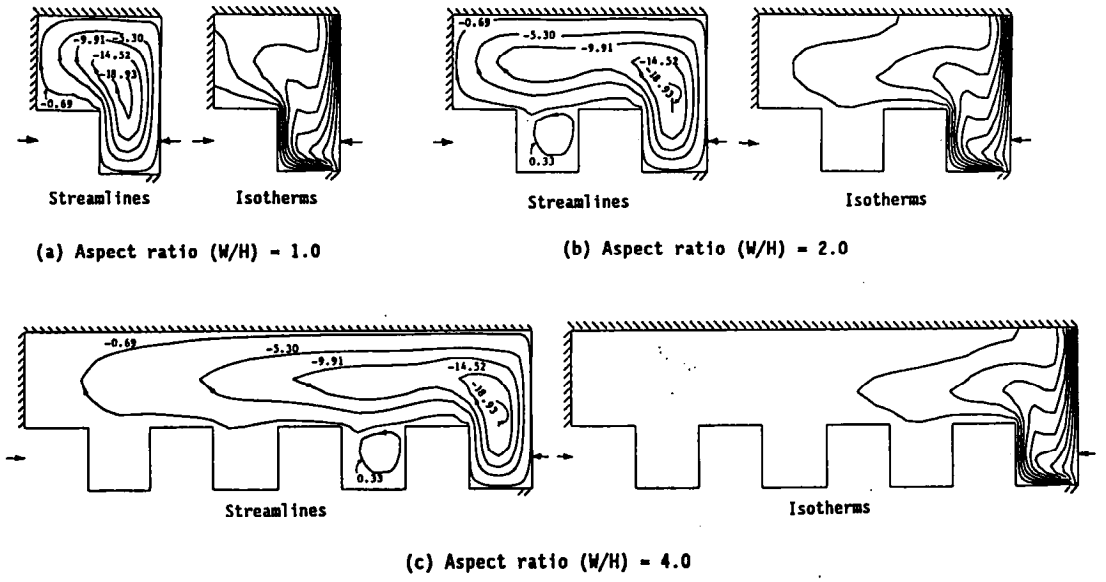

FIG. 7. Computed streamlines and isotherms, $T = 0(0.1)1$, for enclosures with $A = 0.25$, $\delta = 1.0$, $\varepsilon = 0.1$, and $Ra_H = 10^5$.

be compared with curve B, and curve C with curve D. It can be seen that with the increase of amplitude, the ratio of the Nusselt numbers increases. This means that increasing the amplitude increases the heat transfer from the enclosure. To understand this mechanism recall that mounting a periodic array of roughness elements on the bottom wall essentially reduces the effective height of the enclosure. This is because there is little or no thermal activity inside the cavities created by the roughness elements except the one near the cold vertical wall. It is also discussed earlier that at low values of Ra_H (conduction dominated cases), the heat transfer rates across the enclosure are inversely proportional to the effective distance between the hot and cold walls. So, when the amplitude, A, is increased, the effective distance between the hot and cold walls is further decreased; hence, there is more heat transfer. Likewise, it can be said that at high values of Ra_H (convection dominated cases), increasing the amplitude essentially increases the aspect ratio of the enclosure, which is defined in this paper as (width/height). It is already discussed with respect to Fig. 5 that at high values of Ra_H, the heat transfer rate increases with the increase of aspect ratio. Therefore, the increase of heat transfer with the increase of amplitude at high values of Ra_H is expected, because the effective aspect ratio of the enclosure is also increased.

The effect of changing the period, δ, of the roughness elements is also shown in Fig. 8. To study the effect of period from this figure, curve A should be compared with curve C, and curve B with curve D. It can be seen from this figure that with the increase of period, the ratio of Nusselt numbers decreases except at high value of Ra_H (convection dominated case) where the ratio slightly increases. The reason for this trend can be explained by comparing the streamlines and isotherms of Fig. 3(a) with Fig. 6(c) and Fig. 3(c) with Fig. 7(c). Enclosures of these figures have

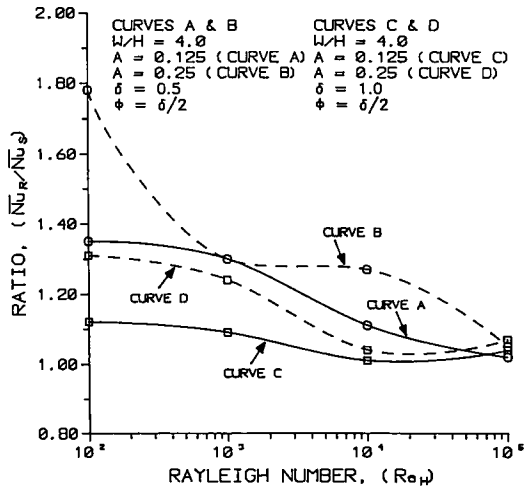

FIG. 8. Effects of amplitude and period on the ratio of Nusselt numbers for enclosures with $Pr = 0.707$.

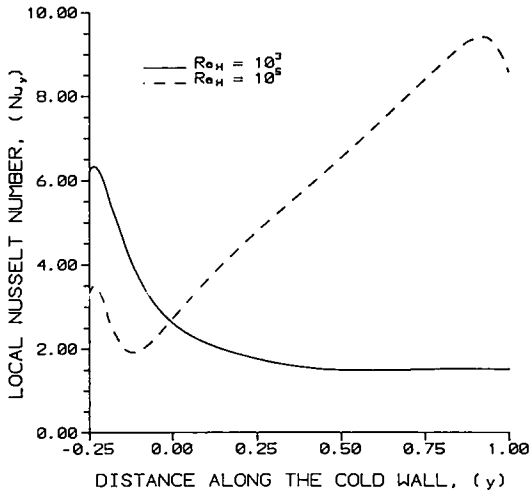

FIG. 9. Local Nusselt number distribution along the cold vertical wall in a rough-walled enclosure with $W/H = 4.0$, $A = 0.25$, $\delta = 1.0$, $\varepsilon = 0.1$, $\phi = \delta/2$, and $Pr = 0.707$.

$W/H = 4.0$, $A = 0.25$, $\varepsilon = 0.1$, and $\phi = \delta/2$. The period of the enclosures of Figs. 3(a) and (c) is 0.5 and the period of the enclosures of Figs. 6(c) and 7(c) is 1.0. From the isotherm contours of these figures it can be seen that in the roughness cavity adjacent to the cold wall, the temperature gradient on the hot wall is higher (identified by the high concentration of isotherms) for an enclosure with $\delta = 0.5$, than that of a corresponding enclosure with $\delta = 1.0$. This gradient is more prominent at the upper left hand corner of the roughness cavity. Since the high temperature gradient increases the heat transfer rate, the Nusselt number ratio (at low values of Ra_H) is higher for the enclosure with smaller period value.

Finally, an important feature for flows in enclosures with present boundary conditions must be noted. From the isotherm contours of Fig. 3(a) (low Ra_H case), a high temperature gradient area is visible at the lower portion of the cold wall. This, of course, suggests that more heat transfer occurs through the lower portion of the cold wall and relatively less heat transfer occurs through the upper portion of the cold wall. However, from the isotherm contours of Fig. 3(c) (high Ra_H case), it is observed that this trend is completely reversed; that is, less heat transfer occurs from the lower portion of the cold wall and more heat transfer occurs from the upper portion of the cold wall. This observation is further illustrated in Fig. 9 where the local Nusselt numbers along the cold vertical wall of a rough-walled enclosure are plotted for high and low values of Ra_H. The opposite nature of local Nusselt number distribution along the cold wall with the increase of Ra_H is quite simple to explain. At low values of Ra_H, conduction is the dominating mode of heat transfer from the hot wall to the cold wall. So, maximum amount of heat will be transferred through the shortest path between these two walls. The lower portion of the cold wall is closest to the hot

wall, so maximum heat transfer is observed there. On the other hand, when Ra_H increases, convection is the dominating mode of heat transfer due to the fluid motion inside the enclosure. Here, cold fluid from the bottom of the cold wall is swept to the left of the enclosure along the hot wall. The fluid then becomes hot and rises towards the top of the enclosure. After reaching the top adiabatic wall, the hot fluid moves to the right towards the cold wall. This hot fluid then comes in contact with the upper portion of the cold wall, so the maximum amount of heat transfer occurs from this first encounter of the hot fluid and the cold wall. Therefore, a higher value of local heat flux is observed at the upper portion of the cold wall for high Rayleigh number flow.

CONCLUSIONS

Based on the parametric study in this research, the following conclusions can be drawn.

(1) The mounting of a periodic array of large rectangular roughness elements on the bottom hot wall of the enclosure of interest in this research increases the rate of heat transfer across the enclosure when the roughness element period, $\phi = \delta/2$. The maximum amount of heat transfer enhancement obtained in this research is 78%. This is obtained for an enclosure with $W/H = 4.0$, $A = 0.25$, $\delta = 0.5$, $\varepsilon = 0.1$, and $\phi = \delta/2$, at $Ra_H = 10^2$ and $Pr = 0.707$.

(2) For phase shift, $\phi = 0$, the ratio of Nusselt numbers $(\overline{Nu}_R/\overline{Nu}_S) < 1$, that is decrement in heat transfer occurs.

(3) With the increase of aspect ratio, heat transfer rates in both smooth-walled and rough-walled enclosures increase at high values of Ra_H. However, at low values of Ra_H, the increase in heat transfer rate becomes constant beyond a critical value of the aspect ratio.

(4) The ratio of Nusselt numbers $(\overline{Nu}_R/\overline{Nu}_S)$ decreases with the increase of Rayleigh number for enclosures with smaller values of roughness element period. For enclosures with higher values of roughness element period, the ratio at first decreases and then increases slightly at high values of Ra_H.

(5) With the increase of the amplitude of the roughness elements, the ratio of Nusselt numbers increases; that is, increment of heat transfer enhancement occurs.

(6) With the increase of the period of the roughness elements, the ratio of Nusselt numbers decreases except at high value of Ra_H, where the ratio increases slightly.

Acknowledgement—This research was partially supported by the Engineering Experiment Station at Montana State University.

REFERENCES

1. R. D. M. Carvalho, L. Goldstein, Jr. and L. F. Milanez, Heat transfer analysis of digital transmission equipment with horizontally arranged printed circuit boards, *Heat Transfer Engng* **9**, 44–53 (1988).
2. K. Torrance and J. Rockett, Numerical study of natural convection in an enclosure with localized heating from below—creeping flow to the onset of laminar instability, *J. Fluid Mech.* **36**, 33–54 (1969).
3. K. Torrance, L. Orloff and J. A. Rockett, Experiments on natural convection in enclosures with localized heating from below, *J. Fluid Mech.* **36**, 21–31 (1969).
4. D. Greenspan and D. Shultz, Natural convection in an enclosure with localized heating from below, *Comput. Meth. Appl. Mech. Engng* **3**, 1–10 (1974).
5. G. S. Shiralkar and C. L. Tien, A numerical study of the effect of a vertical temperature difference imposed on a horizontal enclosure, *Numer. Heat Transfer* **5**, 185–197 (1982).
6. P. Chao, H. Ozoe, S. Churchill and N. Lior, Laminar natural convection in an inclined rectangular box with the lower surface half-heated and half-insulated, *J. Heat Transfer* **105**, 425–532 (1983).
7. S. Kimura and A. Bejan, Natural convection in a differentially heated corner region, *Physics Fluids* **28**, 2980–2989 (1985).
8. D. Poulikakos, Natural convection in a confined fluid-filled space driven by a single vertical wall with warm and cold regions, *J. Heat Transfer* **107**, 867–876 (1985).
9. R. Anderson and G. Lauriat, The horizontal natural convection boundary layer regime in a closed cavity, *Proc. 8th Int. Heat Transfer Conf.*, pp. 1453–1458. San Francisco, California (1986).
10. M. November and M. W. Nansteel, Natural convection in rectangular enclosures heated from below and cooled along one side, *Int. J. Heat Mass Transfer* **30**, 2433–2440 (1987).
11. M. M. Granzarolli and L. F. Milanez, Natural convection in enclosures heated from below and symmetrically cooled from the sides. In *Numerical Simulation of Convection in Electronic Equipment Cooling* (Edited by A. Ortega and D. Agonafer), ASME HTD-Vol. 121, pp. 39–43. San Francisco (1989).
12. M. W. Nansteel, S. S. Sadhal and P. S. Ayyaswamy, Discontinuous boundary temperatures in heat transfer theory, Session on Significant Questions in Buoyancy Affected Enclosure or Cavity Flows, ASME Winter Annual Meeting, December (1986).
13. Z. Y. Zhong, K. T. Yang and J. R. Lloyd, Variable property effects in laminar natural convection in a square enclosure, *J. Heat Transfer* **107**, 133–138 (1985).
14. D. K. Gartling, *NACHOS II—A Finite Element Computer Program for Incompressible Flow Problems, Part I—Theoretical Background*, SAND86-1816, UC-32, Sandia Laboratories, Albuquerque, New Mexico (1987).
15. D. K. Gartling, *NACHOS II—A Finite Element Computer Program for Incompressible Flow Problems, Part II—User's Manual*, SAND86-1817, UC-32, Sandia Laboratories, Albuquerque, New Mexico (1987).